Available online at www.sciencedirect.com

ScienceDirect

Journal of Nuclear Materials 360 (2007) 170–176

journal of nuclear materials

www.elsevier.com/locate/jnucmat

Evaluation of the mitigation effect of hydrogen water chemistry in BWRs on the low-frequency corrosion fatigue crack growth in low-alloy steels

S. Ritter *, H.P. Seifert

Paul Scherrer Institute (PSI), Nuclear Energy and Safety Research Department, Laboratory for Materials Behaviour, 5232 Villigen PSI, Switzerland

Received 3 March 2006; accepted 13 July 2006

Abstract

The mitigation effect of hydrogen water chemistry (HWC) on the low-frequency corrosion fatigue crack growth behaviour of low-alloy steels was investigated under those critical boiling water reactor (BWR) system conditions, where fast corrosion fatigue crack growth significantly above the ASME XI 'wet' reference fatigue crack growth curves was observed under normal water chemistry conditions (NWC). The experiments were performed under simulated BWR conditions at temperatures of 250, 274 or 288 °C. Modern high-temperature water loops, on-line crack growth monitoring (DCPD) and fractographical analysis by scanning electron microscope were used to quantify the cracking response. HWC resulted in a significant drop of low-frequency corrosion fatigue crack growth rates by at least one order of magnitude with respect to NWC conditions and is therefore a promising and powerful mitigation method.

1. Introduction

Both, the accumulated operating experience of low-alloy steel (LAS) primary pressure-boundary components and the experimental/theoretical laboratory background knowledge have basically confirmed the adequacy and conservative character of the ASME XI 'wet' reference fatigue crack growth rate (CGR) curves under most boiling water reactor (BWR)/normal water chemistry (NWC) operating conditions [1–4]. Nevertheless several unfavourable critical combinations of material, loading and environmental parameters, which can lead to accelerated corrosion fatigue (CF) crack growth with CGRs well above the ASME XI 'wet' reference fatigue CGR curves, have been identified in recent research projects at Paul Scherrer Institute (PSI) [2,5]. Hydrogen water chemistry (HWC) with or without noble metal chemical addition (NMCA) is a powerful method to mitigate environmentally-assisted cracking (EAC) in stainless steel and nickel-base alloy components. In both technologies hydrogen is injected into the feedwater to increase the resistance of reactor components to EAC by shifting the electrochemical corrosion potential (ECP) of the components to more negative values.

---

* Corresponding author. Tel.: +41 56 310 2983; fax: +41 56 310 2199.

E-mail address: stefan.ritter@psi.ch (S. Ritter).

0022-3115/$ - see front matter © 2006 Elsevier B.V. All rights reserved.
doi:10.1016/j.jnucmat.2006.07.023

Table 1
Comparison of BWR/NWC and BWR/HWC (NMCA = noble metal chemical addition)

	NWC (≈pure water)	HWC (H_2(>1 ppm) injection into feedwater)	HWC/NMCA (H_2(<0.4 ppm) + noble metal (Pt/Rh) injection into feedwater)
Environment	High ECP/redox potential	Low ECP/redox potential	Low ECP/redox potential
'Negative aspects'	Increased susceptibility to EAC	Increase in shutdown radiation fields, increase in main steam line radiation levels, high amount of H_2	(Increase in shutdown radiation fields), interaction of the noble metal with the fuel (?)
'Positive aspects'		Reduced susceptibility to EAC	Reduced susceptibility to EAC, less H_2 necessary
Application	≈45% of the BWR plants worldwide (ca. 40 BWR plants)	≈55% of the BWR plants worldwide (ca. 20 BWR plants HWC, ca. 30 BWR plants HWC/NMCA)	

In Table 1 HWC is briefly compared with NWC and some of the basic advantages and disadvantages are shown. A growing number of BWR plants (ca. 55% of the BWR plants worldwide) are using these technologies. Although the mitigation effect of HWC has been mainly investigated with stainless steels and nickel-base alloys so far [6,7], a very beneficial effect is also expected for LASs. Therefore a research project was started at PSI (RIKORR-II) [8] to evaluate the mitigation effect of HWC on the crack growth behaviour of low-alloy reactor pressure vessel (RPV) steels and to get a reliable quantitative EAC CGR database for flaw tolerance evaluations and assessments of safety margins. The present paper summarizes some of the major results of these preliminary investigations.

2. Materials and experimental procedure

2.1. Materials and specimens

Several different types of low-alloy, nuclear grade RPV steels were investigated (see Table 2). Concerning the EAC behaviour, the steels mainly differ in their susceptibility to dynamic strain ageing (DSA), sulphur content/MnS morphology and yield stress.

All RPV steels were quenched and tempered. Some materials were post-weld heat-treated or stress relieved. The alloys had a granular, bainitic (alloy A, C, D, E) or a mixed bainitic/ferritic-pearlitic structure (alloy B) with an average former austenitic grain size of 10–20 μm. The spatial distribution and morphology of the MnS inclusions was fairly homogeneous and similar in alloys A–D covering the range from small, spherical to large (up to a few 100 μm), elongated inclusions. Alloy E revealed distinct banded sulphur segregation zones with large clusters of MnS inclusions.

Twenty-five millimeters thick compact tension specimens (1T-C(T)) according to ASTM E399 were used for all experiments. The specimens were manufactured from the forged ingots or hot-rolled steel plates mainly in T–L or L–T orientation. The specimens were pre-cracked by fatigue in air at room temperature, using a load ratio R of 0.1. The maximal K_I at the final load step was $\leqslant 15$ MPa m$^{1/2}$.

2.2. Experimental procedure

The EAC tests were performed in 10 l stainless steel autoclaves with integrated electromechanical loading systems, which were attached to sophisticated refreshing high-temperature water loops (see Fig. 1). During the experiments all important mechanical (load, pull rod stroke) and environmental parameters at inlet and outlet (dissolved oxygen (DO), dissolved hydrogen (DH), conductivity κ, temperature, pressure, flow) were recorded continuously. The ECP of the specimens and the redox potential (platinum probe) were continuously monitored by use of an external Ag/AgCl/0.01 M KCl or $Cu/Cu_2O/ZrO_2$-membrane reference electrode. Ionic impurities of the water (inlet and outlet) were analyzed by inductive coupled plasma-atomic emission spectroscopy (ICP-AES) and ion chromatography (IC) about four times each test. Usually, two air fatigue pre-cracked 1T-C(T) specimens were simultaneously tested in a 'daisy chain'. Before applying the different loading sequences, the specimens were pre-oxidized in the test environment at a small constant pre-load for one week. The crack advance was monitored using the reversed direct current potential drop (DCPD) method with a resolution limit of about 2–5 μm. After the tests all specimens were broken open at liquid nitrogen temperature for fractographical analysis in the scanning electron microscope.

Table 2
Overview on investigated low-alloy RPV steels (WQ = water quenched, FC = furnace cooled, AC = air cooled, SR = stress relief heat-treatment, DSA = dynamic strain ageing: +++: high, ++: medium, +: low DSA susceptibility)

Material		S (wt%)	Al (wt%)	N_{free} (ppm)	Heat treatment	Microstructure	$R_P^{288°C}$ [MPa]	DSA
20 MnMoNi 5 5 (≡SA 508 Cl.3)	A	0.004	0.013	30	910–920 °C/6 h/WQ 640–650 °C/9.5 h/FC	Bainitic	418	+++
SA 508 Cl.2 (≡22 NiMoCr 3 7)	B	0.004	0.015	2	900 °C/ 8 h/WQ 600 °C/9 h/AC	Bainitic/ ferritic-pearlitic	396	+++
SA 533 B Cl.1 (≡20 MnMoNi 5 5)	C	0.018	0.030	<1	915 °C/12 h/AC/860 °C/12 h/WQ 660 °C/12 h/FC/610 °C/40 h/FC 550 °C/12 h/FC/550 °C/12 h/FC	Bainitic	412	++
22 NiMoCr 3 7 (≡SA 508 Cl.2)	D	0.007	0.018	3	890–900 °C/7 h/WQ 640–650 °C/17 h/AC+SR	Bainitic	400	+
20 MnMoNi 5 5 (≡SA 508 Cl.3)	E	0.015 (0.003–0.053)	0.029	?	900 °C/9 h/WQ/650 °C/34 h/AC 660 °C/14 h/AC/550 °C/47 h 600 °C/8 h/AC	Bainitic	439	++

The cyclic loading in the CF tests was performed under load control. Constant load amplitude loading with a positive saw tooth waveform (slow loading, fast unloading) was applied. The rise time Δt_R, load ratio R and load level were varied over a very broad range. In most cases the $K_{I,max}$ values were below the ASTM E647 limit for linear elastic conditions.

BWR conditions were mostly simulated with high-purity (inlet/outlet conductivity κ of <0.06/ < 0.1 μS/cm), hydrogenated (HWC) or oxygenated (NWC) water at a temperature of 274 or 288 °C. For HWC conditions, a DH content of 0.15 ppm was usually applied. For NWC conditions a DO content of 0.4 or 8 ppm was used. The water chemistry conditions and resulting ECP and redox potential for a temperature of 288 °C are summarized in Table 3. The increased DO value of 8 ppm (ECP = + 150 mV_{SHE}, redox potential = + 290 mV_{SHE}) was applied additionally to either simulate plant transients (e.g., start-up) and locations with oxygen enrichment (e.g., piping with stagnant steam non-degassed condensate) or to achieve a realistic ECP of +150 mV_{SHE} for a surface crack penetrating the stainless steel cladding on the RPV wall/nozzles. These conditions may appear to be overly aggressive/conservative for many other LAS BWR pressure boundary components (e.g., feedwater piping or piping with flowing steam). To simulate transient BWR power operating conditions, additional tests at a temperature of 250 °C were performed as well as sulphate or chloride were added to the high-purity water in some experiments. All tests were performed under low-flow conditions (4–5 autoclave exchanges per hour) with a local flow rate of some few mm/s to generate conservative data with respect to most plant locations with turbulent high-flow conditions.

3. Results and discussion

3.1. *Corrosion fatigue crack growth under BWR/NWC conditions*

The adequacy and conservative character of the current ASME XI 'wet' reference fatigue crack growth curves under BWR/NWC conditions have been evaluated over a wide range of environmental (T, ECP/DO, SO_4^{2-}, Cl^-), loading (v, ΔK, R) and material (S, MnS, microstructure) parameter combinations at PSI and have been discussed in detail in a recent conference paper [2]. The observed CF

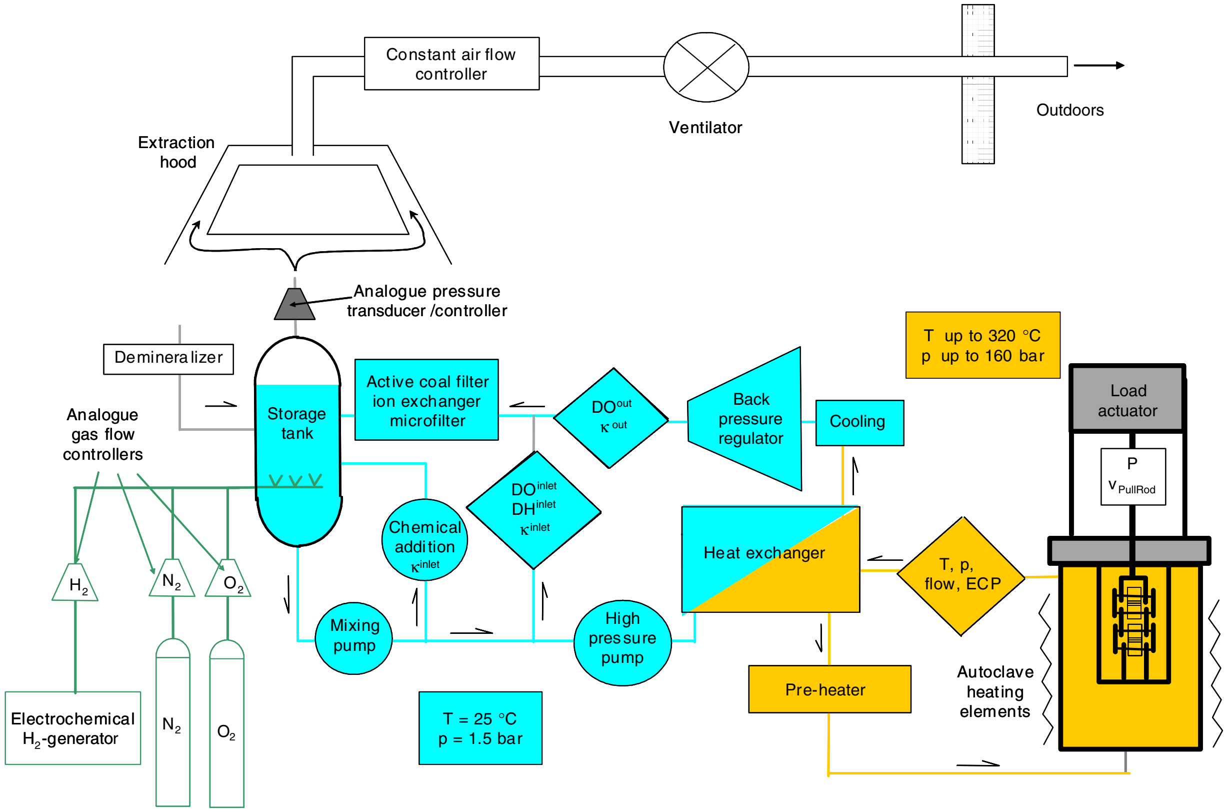

Fig. 1. Schematic of a high-temperature water loop with autoclave and electro-mechanical tensile machine.

Table 3
Simulated BWR/NWC and BWR/HWC conditions (DO = dissolved oxygen content, DH = dissolved hydrogen content, ECP = electrochemical corrosion potential)

	DO (ppm)	DH (ppm)	ECP (mV_{SHE})	Redox (mV_{SHE})
NWC	0.40	0.00	+40 to +60	+250
	8.00	0.00	+130 to +170	+290
HWC	0.00	0.15	−550 to −620	−530

crack growth behaviour is exemplarily shown in Figs. 2 and 3. The current ASME XI ‘wet’ reference fatigue CGR curves conservatively covered the CF CGR lab data under most simulated BWR/NWC conditions and parameter combinations, and were usually only exceeded under some very specific BWR plant conditions. In particular under highly oxidizing BWR/NWC conditions ($+50 \leqslant \mathrm{ECP} \leqslant +200\ \mathrm{mV_{SHE}}$, 0.4–8 ppm DO), the current ASME XI ‘wet’ reference fatigue CGR curves could be significantly exceeded for all investigated materials in the temperature range between 150 and 288 °C by cyclic fatigue loading at low frequencies $\nu \leqslant 10^{-2}$ Hz and $\Delta K > 5\ \mathrm{MPa\ m^{1/2}}$ or at $10^{-2}\ \mathrm{Hz} < \nu < 10\ \mathrm{Hz}$ and high $R \geqslant 0.9$/small $\Delta K \leqslant 5\ \mathrm{MPa\ m^{1/2}}$ (ripple loading). Fast CF crack growth could be sustained down to very low frequencies of

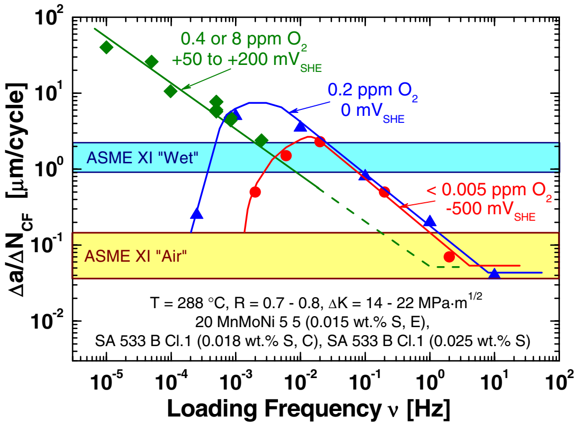

Fig. 2. Effect of DO/ECP and loading frequency on $\Delta a/\Delta N_{\mathrm{CF}}$ and comparison to corresponding ASME XI reference fatigue CGRs for the specified loading conditions. Data at < 0.005 ppm DO are taken from Atkinson et al. [9].

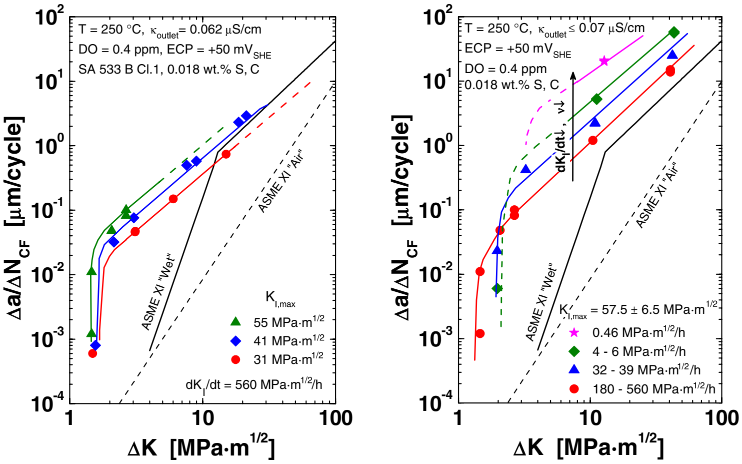

Fig. 3. Effect of ΔK (left) and loading rate dK_I/dt (right) on $\Delta a/\Delta N_{CF}$ in material C for increasing load ratio/decreasing ΔK-tests at constant $K_{I,max}$ and dK_I/dt and comparison to the corresponding ASME XI reference fatigue CGR curves for the specified loading conditions.

3×10^{-6} Hz (see Fig. 2) and ΔK values $\geqslant 2$ MPa m$^{1/2}$ (see Fig. 3). Under moderately oxidizing BWR/NWC conditions (ECP = −100 to 0 mV$_{SHE}$, 0.05–0.2 ppm DO), at $\Delta K > 5$ MPa m$^{1/2}$ the curves were usually only exceeded in a relatively narrow frequency range of 10^{-4}–10^{-2} Hz (see Fig. 2) [2].

3.2. Corrosion fatigue crack growth under BWR/HWC conditions

The mitigation effect of HWC on CF crack growth was investigated under those critical combinations of material, loading and environmental parameters, which lead to fast CF with CGR well above the ASME XI 'wet' reference fatigue CGR curves under NWC conditions (see Section 3.1).

CF tests at PSI with NWC (0.4 or 8 ppm DO) → HWC (0.15 ppm DH) → NWC-transients always revealed a significant drop of the CF CGR (by a factor of 10–50) under low-frequency fatigue loading conditions ($\leqslant 0.01$ Hz) a few hours after adding hydrogen and changing to low potential conditions (< -200 mV$_{SHE}$). A few 10 hours after returning to oxidizing NWC conditions, the CF CGR again reached the same range of (accelerated) 'high-sulphur' CF CGR as before the HWC-transient. This is exemplarily shown in Fig. 4. At very low loading frequencies, the CF CGR remained on the low HWC level after returning back to NWC conditions and the accelerated 'high-sulphur' CF CGR could only be re-established after a temporary increase of loading frequency.

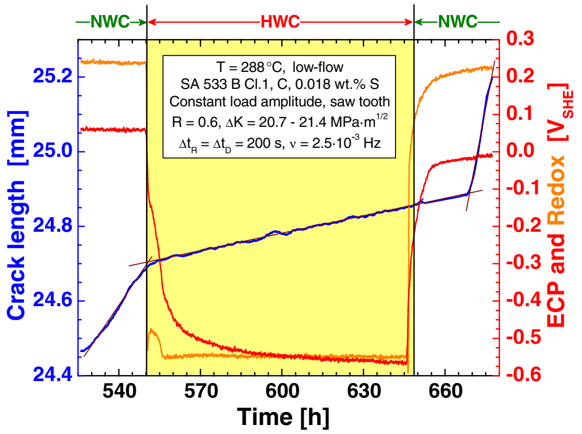

Fig. 4. Example of low-frequency CF crack growth during a NWC → HWC → NWC-transient.

In Fig. 5, the PSI results at different loading conditions are compared to similar investigations of Andresen and Young [10] including noble metal coated specimens [11] and to the predictions of the GE-model [12]. By changing from oxygenated (or stoichiometric excess of oxygen in case of NMCA) to hydrogenated (or stoichiometric excess of hydrogen in case of NMCA) water chemistry conditions, the CF CGRs always dropped from the 'PSI NWC CF regression curve', which is close to the 'high-sulphur' CF curve, down to the 'low-sulphur' CF CGRs of the GE-model. HWC/NMCA resulted in a significant reduction of CF CGRs by a factor of 10–50 under the tested low-frequency loading conditions, where ASME XI 'wet' reference fatigue

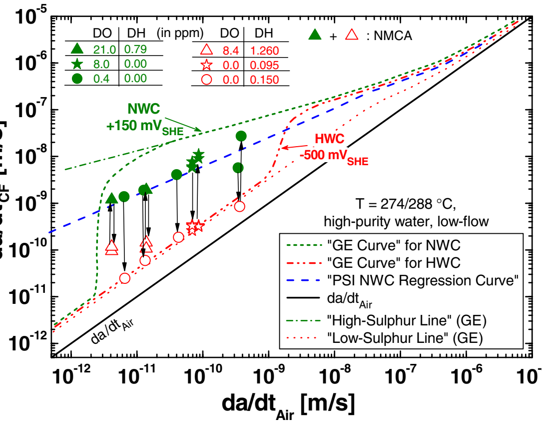

Fig. 5. Reduction of time-based CF CGRs da/dt_{CF} by changing from NWC to HWC/NMCA (NMCA-data from Andresen and Angeliu [11]) and comparison with the 'high-sulphur' and 'low-sulphur lines' of the GE-model [12].

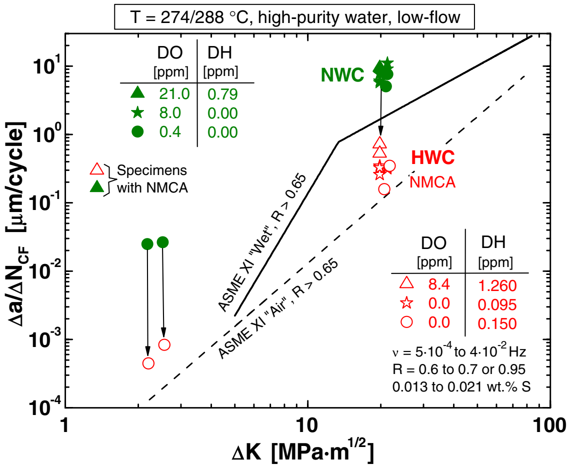

Fig. 6. Comparison of stationary low-frequency CF CGRs $\Delta a/\Delta N_{EAC}$ during NWC and HWC/NMCA phases with the corresponding ASME XI reference fatigue CGR curves (NMCA-data from Andresen and Angeliu [11]).

CGRs were significantly exceeded under NWC conditions (see Fig. 6). On the other hand, no or only a very moderate reduction of CF CGRs by HWC is expected above a loading frequency of 10^{-2}–10^{-1} Hz (see Figs. 2 and 5), since 'high-sulphur' crack-tip environment conditions may also prevail in this frequency range in deoxygenated high-temperature water (by the exposure and dissolution of new fresh MnS-inclusions by the fast growing crack and the relatively slow transport of the sulphides out of the crack by diffusion).

In Fig. 6 the stationary low-frequency (5×10^{-4}–4×10^{-2} Hz) cyclic CF CGRs $\Delta a/\Delta N_{CF}$ during NWC and HWC/NMCA phases are compared to the ASME XI reference fatigue crack growth curves. Under these conditions, $\Delta a/\Delta N_{CF}$ significantly exceeded the ASME XI 'wet' reference fatigue CGR curve under NWC conditions, but dropped well below this curve under HWC conditions. Thus HWC or HWC/NMCA seem to be very promising methods to reduce low-frequency CF CGRs.

4. Summary and conclusions

The mitigation effect of BWR/HWC on the low-frequency CF crack growth behaviour of low-alloy RPV steels was investigated. The special emphasis was placed to those critical parameter combinations, which revealed accelerated CF crack growth well above the ASME XI 'wet' reference fatigue crack growth curves under NWC conditions in previous studies. For this reason, the CF crack growth behaviour of different RPV steels in oxygenated (NWC) or hydrogenated (HWC) high-temperature water was characterized by cyclic load tests with pre-cracked fracture mechanics specimens. The application of HWC always resulted in a significant reduction of low-frequency CF CGRs by at least one order of magnitude with respect to NWC conditions. A few hours after changing from oxidizing NWC to reducing HWC conditions, the CGRs dropped below the corresponding disposition curves. HWC is therefore a promising and powerful mitigation method for EAC in LAS under those critical parameter combinations.

It is recommended to further verify these promising results by tests in the ECP range from −500 to −200 mV_{SHE} and at different hydrogen to oxygen concentration ratios including experiments with noble metal coated specimens to cover the whole BWR/HWC or HWC/NMCA operation range.

Acknowledgements

This work has been performed within the RI-KORR-I/II projects. The financial support for this work by the Swiss Federal Nuclear Safety Inspectorate (HSK) and the Swiss Federal Office of Energy (BFE) is gratefully acknowledged. Thanks are also expressed to U. Ineichen, B. Gerodetti, U. Tschanz and E. Groth (all PSI) for their experimental contribution to the projects.

References

[1] H.P. Seifert, S. Ritter, J. Hickling, Power Plant Chem. 6 (2004) 111.

[2] H.P. Seifert, S. Ritter, in: Proceedings of the Third International Conference on Fatigue of Reactor Components, Session 3: Environmental Effects, Seville, Spain, October 3–6, 2004.

[3] P. Scott, D. Tice, Nucl. Eng. Design 119 (1990) 399.

[4] Y.S. Garud et al., Corrosion fatigue of water-touched pressure retaining components in power plants, EPRI TR-106696, Final Report, November 1997.

[5] S. Ritter, H.P. Seifert, Power Plant Chem. 5 (2003) 17.

[6] P.L. Andresen, T.P. Diaz, S. Hettiarachchi, in: Proceedings of the NACE Corrosion 2004, Paper No. 04668, NACE, New Orleans, LA, USA, 2004.

[7] R.L. Cowan, Water chemistry of nuclear reactor systems, 1 (1996), BNES, 196.

[8] H.P. Seifert, S. Ritter, U. Ineichen, U. Tschanz, B. Gerodetti, Risskorrosion in druckführenden Komponenten des Primärkreislaufes von SWR, BFE Annual Report 2004, PSI, Switzerland, November 2004.

[9] J.D. Atkinson, J. Yu, Z.J. Zhao, in: Proceedings of the Seventh International Conferences on Environment Degradation of Materials in Nuclear Power Systems – Water Reactors, ANS/TMS/NACE, Amelia Island, USA, 1997, p. 924.

[10] P.L. Andresen, L.M. Young, Corrosion 51 (1995) 223.

[11] P.L. Andresen, T.M. Angeliu, in: Proceedings of the NACE Corrosion 1996, Paper No. 969084, NACE, Houston, TX, USA, 1996.

[12] F.P. Ford, P.L. Andresen, in: W. Cullen (Ed.), Proceedings of the Third International IAEA Specialist's Meeting on Sub-critical Crack Growth, NUREG/CP-0112, Moscow, USSR, May 14–17, 1990, vol. 1, p. 105.